Detection of Olfactory Stimulus in Electroencephalogram Signals Using Machine and Deep Learning Methods

Burak Akbugday[1] , Sude Pehlivan Akbugday[2] , Riza Sadikzade[1] , Aydin Akan[1] , Sevtap Unal[3]

[1]Department of Electrical and Electronics Engineering, Izmir University of Economics Faculty of Engineering, Izmir, Balcova, Turkey
[2]Department of Biomedical Engineering, Izmir University of Economics Faculty of Engineering, Izmir, Balcova, Turkey
[3]Department of International Trade and Business, Izmir Katip Celebi University Faculty of Economics and Administrative Sciences, Izmir, Turkey

ABSTRACT

The investigation of olfactory stimuli has become more prominent in the context of neuromarketing research over the last couple of years. Although a few studies suggest that olfactory stimuli are linked with consumer behavior and can be observed in various ways, such as via electroencephalogram (EEG), a universal method for the detection of olfactory stimuli has not been established yet. In this study, 14-channel EEG signals acquired from participants while they were presented with 2 identical boxes, scented and unscented, were processed to extract several linear and nonlinear features. Two approaches are presented for the classification of scented and unscented cases: i) using machine learning (ML) methods utilizing extracted features; ii) using deep learning (DL) methods utilizing relative sub-band power topographic heat map images. Experimental results suggest that the olfactory stimulus can be successfully detected with up to 92% accuracy by the proposed method. Furthermore, it is shown that topographic heat maps can accurately depict the response of the brain to olfactory stimuli.

Index Terms— Deep Learning, electroencephalogram (EEG), machine learning, neuro-marketing, olfactory stimulus

I. INTRODUCTION

Consumer behavior highly depends on the emotional state of a person. Emotion can be defined as mental experiences with high hedonic content and high intensity [1]. Different biological signals, such as the electroencephalogram (EEG), provide vital information about the emotional state of the person. The reward estimate, which is associated with the orbitofrontal cortex, is one of the major components of purchase intention [2]. Several studies on attention, mood, and personal preferences were conducted on the human brain. Several imaging and signal acquisition methods, such as EEG, are currently utilized to investigate the brain. An EEG is a suitable technique for investigating phenomena connected to neuromarketing since it has a high temporal resolution, is inexpensive, and is noninvasive [3]. Olfactory stimulus is currently being studied extensively as it affects the process of making a purchase decision by altering the emotions of people.

Seet et al. [2] examined consumer behavior using four fragrances on 14 volunteers. Approximate entropy (ApEn) and relative power spectral Density (PSD) of the EEG sub-bands were used with several machine learning (ML) algorithms, and the combination of these two features achieved 75.9% accuracy for the binary classification.

Ezzatdoost et al. [4] utilized EEG signals to distinguish pleasant and unpleasant scents. The features utilized for subject-specific and cross-subject classification include Lempel–Ziv complexity (LZC), largest Lyapunov exponent (LLE), ApEn, and Higuchi's fractal dimension (HFD). Using the entire feature set improved accuracy for both classification scenarios, and the eyes-open condition was determined to be superior to the eyes-closed condition.

Hou et al. [5] assessed various emotions, such as pleasure and disgust, by using different odors on 11 participants. Welch's method was utilized to derive PSD features based on EEG rhythms from each participant's 35 trials for 13 fragrances. The Support Vector Machine (SVM) outperformed

the other classifiers with a 98.9% accuracy rate. Afterward, classes were increased to 5, and although less precise, an accuracy of 88.5% was adequate [5].

Many researchers [6–8] used nonlinear and linear features that can be extracted from the EEG signals, including higher-order moments in the time and frequency domains, differential entropy, Hjorth parameters (HPs), Lyapunov exponent, EEG sub-band powers, detrended fluctuation analysis, fractal dimension (FD), and LZC [4]. To identify olfactory cues, researchers have used these nonlinear characteristics in the EEG data. Kroupi et al. [9] employed a linear discriminant analysis (LDA) classifier to detect odor pleasantness using permutation entropy (PE) and minimum cover (MC) dimension features and achieved accuracy rates of up to 90% in some circumstances, with a mean accuracy of 53.89% for MC and 56.16% for PE features. Aydemir [10] employed linear and statistical characteristics, as well as nonlinear features, to classify odors and subjects using multiple ML methods. Auto-regressive, statistical, and band power features performed better under certain situations, reaching up to 96.94% for the four-odor classification, respectively. Ezzatdoost et al. [4] classified four odors and pleasantness using nonlinear characteristics and ML classifiers and obtained 64.3% and 54.8% accuracy in odor recognition [4].

Throughout the years, several classification methods have been proposed, including SVM, LDA, Bayesian classifiers, and k-nearest neighbors (k-NN). However, as publicly available datasets with huge amounts of experimentally obtained EEG signals became available, researchers began to employ deep learning (DL) techniques [11]. The widely used DL approaches in emotion recognition tasks are deep belief networks (DBN), multi-layer perceptron neural networks (MLPNN), convolutional neural networks (CNN), and recurrent neural networks (RNN) [12]. Recently, several studies have stated that the CNN approach is highly successful in feature extraction and classification tasks [13-16].

Rahman et al. utilized a CNN model on the Emotion EEG Dataset (SEED) dataset by giving topographic pictures of EEG data as input to classify emotions. Topographic images were obtained from the Relative PSD. Three emotional states—positive, negative, and neutral—were classified. The results showed that an average accuracy of 89% was obtained [15].

The main drawback of the studies in the state of the art is that authors utilize public datasets, which often include very few participants, such as [4], [9], and [10]. In this study, the dataset was created by obtaining EEG signals from 33 participants while they were presented with olfactory stimuli by presenting scented and unscented versions of the identical product packaging. Nonlinear characteristics such as HFD [17], HPs [18], and LZC [19] were utilized to examine their effectiveness in olfactory stimuli classification and the analysis of emotional processes using EEG signals [4]. The performance of ML classifiers was tested using different metrics and compared with the authors' previous work, which was conducted using the same dataset but used PSDs of the EEG sub-bands [20]. The main contribution of this study is to compare the effectiveness of various linear and nonlinear features to classify the olfactory stimuli from EEG signals to highlight the better-performing features. The second contribution of the paper is the utilization of a CNN classifier that uses the heat map of relative sub-band powers to indicate the presence of olfactory stimuli more consistently, as the accuracy of the ML-based classifiers vastly differs depending on the parameters and classification algorithms used.

II. MATERIALS AND METHODS

A. Experimental Setup
The EEG recordings were obtained from randomly chosen 20 male and 13 female volunteers at Izmir University of Economics, Department of Electrical and Electronics Engineering. Subjects were recruited from various ages and social and economic backgrounds. An informed consent form was read and signed by the subjects before they were included in the experiment. None of the subjects indicated that they had conditions that would require them to be excluded from the study. The acquisition was done over 14 different channels using a widely accepted 10–20 electrode placement technique, which can be seen in Fig. 1. EMOTIV EPOC+ was used with a 256 Hz sampling rate.

The experiment included two steps, as given in detail in [21], the first being an EEG recording and the second being a questionnaire. Two online market sites provided participants with 2 open boxes of identical products, one of which was scented with a perfume and the other unscented. Following each product, a questionnaire was distributed to conduct a satisfaction study. Although the recording setting was silent, the participants' ears were covered to prevent aural inputs. Participants were instructed not to move their hands or talk. Furthermore, with the help of a barrier, participants' visual fields were blocked to prevent visual interference.

All the feature extraction and classification steps were done using Python and related packages.

B. Feature Extraction
In this study, to identify the presence of olfactory stimuli in the EEG recordings,

i)   several nonlinear features such as HFD, LZC, Hjorth complexity (HC), Hjorth activity (HA), and Hjorth mobility (HM) and
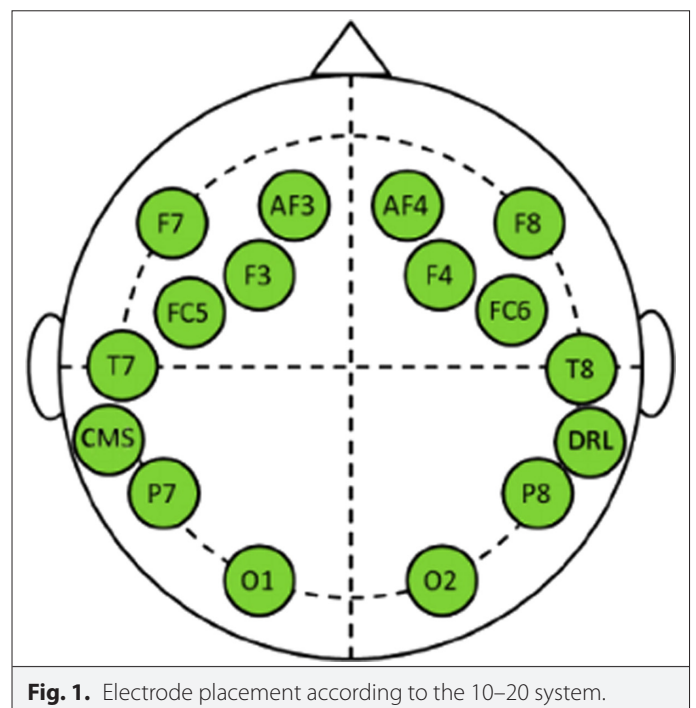ii) relative sub-band powers of EEG are utilized.

Fig. 1. Electrode placement according to the 10–20 system.

These features were previously used by other researchers in previous studies. Features such as PSD [2], LZC, LLE, HFD [4], and other various linear and nonlinear features in [6–8] were exploited since they can expose the subtle but valuable changes in the EEG signal when an olfactory stimulus is present. Furthermore, these features can indicate which regions of the brain are more active by analyzing and correlating the EEG recordings from different channels.

1) Higuchi's Fractal Dimension

It is a time domain feature and a nonlinearity measure of the complexity of waveforms. As discrete signals can either be examined as a sequence or time series, it is possible to determine the curve length $L_m(k)$ for each series using (1), where N stands for the length of the signal X, and $\dfrac{N-1}{\left[\dfrac{N-m}{k}\right]k}$ denotes the normalization factor.

$$L_m\left(k\right)=\frac{1}{k}\left(\sum_{i=1}^{\left[\frac{N-m}{k}\right]}\left|X\left(m+ik\right)-X\left(m+\left(i-1\right)k\right)\right|\frac{N-1}{\left[\frac{N-m}{k}\right]k}\right) \tag{1}$$

The mean of the curve length $L(k)$ is obtained by averaging $L_m(k)$ for all m in the manner described in (1). The HFD is calculated as the least squares polynomial fit of ln$k$, where ln denotes the natural logarithm, and ln$L(k)$, after computation and array formation of all $L(k)$ values [22].

The procedure requires the use of a suitable maximum value for k_{max}, as it modifies the calculated FD [23]. Several researchers, such as [24, 25], proposed plotting HFD values against a range of conceivably appropriate k_{max} values to determine where the plot plateaus to choose an appropriate value. It is considered that the plateau point represents the saturation point and a suitable value. As a result, different HFDs were computed using various k_{max} values, and it was determined that $k_{max} = 14$ is the most suitable.

2) Lempel–Ziv Complexity

This feature calculates the signal's temporal complexity [19]. To calculate LZC, first, a binary sequence is constructed using (2).

$$s\left(n\right)=\begin{cases}0, x\left(n\right)>M\\1, x\left(n\right)<M\end{cases} \tag{2}$$

The binary sequence is polled left-to-right to obtain unique sequences. Afterward, complexity is calculated using (3). α indicates the number of different symbols, and $c(N)$ depicts a counter that increases gradually as a distinct sequence is detected in (3) [4].

$$b\left(N\right)=\lim_{N\to\infty}c\left(N\right)=\frac{N}{\log N} \tag{3}$$

3) Hjorth Parameters

Computation of the time complexity of signals is done via HPs. Equations (4), (5), and (6) are used to calculate the HPs, which are HA, HM, and HC, respectively [26].

$$Activity=Var\left(y\left(t\right)\right) \tag{4}$$

$$Mobility=\sqrt{\frac{Var\left(\dfrac{d\left(y\left(t\right)\right)}{dt}\right)}{Var\left(y\left(t\right)\right)}} \tag{5}$$

$$Complexity=\sqrt{\frac{Mobility\left(\dfrac{d\left(y\left(t\right)\right)}{dt}\right)}{Mobility\left(y\left(t\right)\right)}} \tag{6}$$

In (4) and (5), $Var(y(t))$ depicts the variance of $y(t)$. In (5) and (6), it $\dfrac{d\left(y\left(t\right)\right)}{dt}$ depicts the first derivative of $y(t)$.

4) Electroencephalogram Relative Sub-band Powers

The sub-band powers of EEG segments were utilized as another set of features for the classification of scented and unscented cases. The PSD of the EEG segments is estimated by using the Welch periodogram approach [20] given in (7) and (8).

$$\check{P}^i\left(f_k\right)=\frac{T_s}{M}\left|\sum_{n=0}^{M-1}x_i\left(n\right)w\left(n\right)e^{-2\pi f_k n}\right|^2 \tag{7}$$

Here i indicates the segment number, T_s is the scaling factor, and $f_k=\dfrac{k}{M}, k=0,1,\dots,M-1$ are the frequency samples. The signal $x(n)$ is windowed to form overlapping sections by the window function $w(n)$. Discrete Fourier transform of the L segments was obtained first, and then the average was calculated to form the Welch PSD estimate as:

$$\check{P}_W\left(f_k\right)=\frac{1}{L}\sum_{i=0}^{L-1}\check{P}^i\left(f_k\right) \tag{8}$$

Then periodograms are used to identify the power contained in the following sub-bands of EEG: δ (0.5–4 Hz), θ (4–8 Hz), α (8–13 Hz), β (13–30 Hz), and γ (30–40 Hz), i.e., P_δ, P_θ, P_α, P_β, and P_γ, which are calculated as (9):

$$P_{sb}=\sum_{f_k\in f_{sb}}\check{P}_W\left(f_k\right),\quad sb=\left\{\delta,\theta,\alpha,\beta,\gamma\right\} \tag{9}$$

where f_{sb} is a subset of frequencies corresponding to the related sub-band $sb=\{\delta,\theta,\alpha,\beta,\gamma\}$. The total power P_T in each channel is also calculated as (10).

$$P_T=\sum_{f_k}\check{P}_W\left(f_k\right) \tag{10}$$

Each sub-band's relative power is estimated via the division of the sub-band power by the total channel power [27] as (11).

$$P_{sb}^r=\frac{P_{sb}}{P_T},\quad sb=\left\{\delta,\theta,\alpha,\beta,\gamma\right\} \tag{11}$$

The relative sub-band powers P_{sb}^r of each channel are used in two classification approaches in this proposed study.
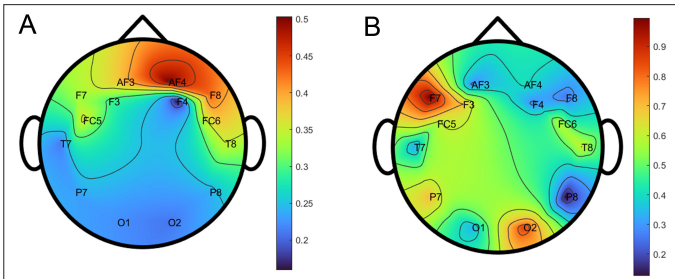
Fig. 2. (a) Heat map for the theta sub-band of a channel of one subject for the unscented case. (b) Heat map for the theta sub-band of a channel of one subject for the scented case.

1. To train traditional classifiers such as k-NN, NB, SVM, and Random Forest (RF).
2. To generate topographic heat map images that are used to train a CNN.

for the classification of the EEG segments from scented and unscented experiments. The heat map approach was adopted from [28], and the algorithm utilizes interpolation to 81 electrode positions for a 10–20 electrode system. Fig. 2 depicts the heat maps for the θ sub-band of a channel of one subject for scented and unscented cases.

C. Classification
In this study, both i) ML methods using the extracted features and ii) a DL method using topographic heat map images generated from the relative sub-band features to classify the EEG segments of scented and unscented cases were used.

1. **Classification via Machine Learning Methods:** Feature matrices were split into train and test sets following an 80%–20% convention, respectively. To classify olfactory stimuli, gradient boost (GB), naïve Bayes (NB), k-NN, decision tree (DT), SVM, and RF-ML algorithms were used. Extracted features were utilized to train models for each and all EEG channels, both individually and collectively. After using the default classifier parameters of the algorithms, grid search was employed to tune the hyperparameters to improve the performance of the classifiers. All the classifiers use 10-fold cross-validation of train and test data.
2. **Classification via Deep Learning:** In the second approach, a CNN architecture was utilized to classify the topographic heat

map images of the sub-band power features, which were first normalized according to (12). The generated heat maps were concatenated into groups of four. Since the combination of sub-bands was random, the concatenation process was performed blindly. Instead of using each band power of each subject for all channels separately, it is proposed in this study to increase the number of data points using concatenation. Examples of concatenated sub-band heat map images are given in Fig. 3.

The CNN architecture includes two convolutional layers, where both layers are followed by the max-pooling layers. The kernel sizes of the convolutional layers were chosen as 3, the Rectified Linear Unit activation function was used. After flattening, a dense layer was implemented, which was followed by a dropout layer with a 0.5 dropout ratio. The last layer was a dense layer with a sigmoid activation function. The total architecture can be seen in Table I.

$$x' = \frac{x - \min(x)}{\max(x) - \min(x)} \tag{12}$$

D. Classification Metrics
Several performance metrics were utilized to compare classifier performances; these metrics include measures that show an accurate prediction of the existence of olfactory stimuli. True negatives (TN), true positives (TP), false negatives (FN), and false positives (FP) were used to calculate accuracy, precision, recall, and F1-score, which are the measures utilized for assessment. To obtain these metrics, (13), (14), (15), and (16) are used, respectively.

$$\text{Accuracy} = \frac{TP + TN}{TP + TN + FP + FN} \tag{13}$$

$$\text{Precision} = \frac{TP}{TP + FP} \tag{14}$$

$$\text{Recall} = \frac{TP}{TP + FN} \tag{15}$$

$$F-1\text{Score} = \frac{2\left(\frac{TP}{TP+FP}\right)\left(\frac{TP}{TP+FN}\right)}{\left(\frac{TP}{TP+FP}\right) + \left(\frac{TP}{TP+FN}\right)} \tag{16}$$
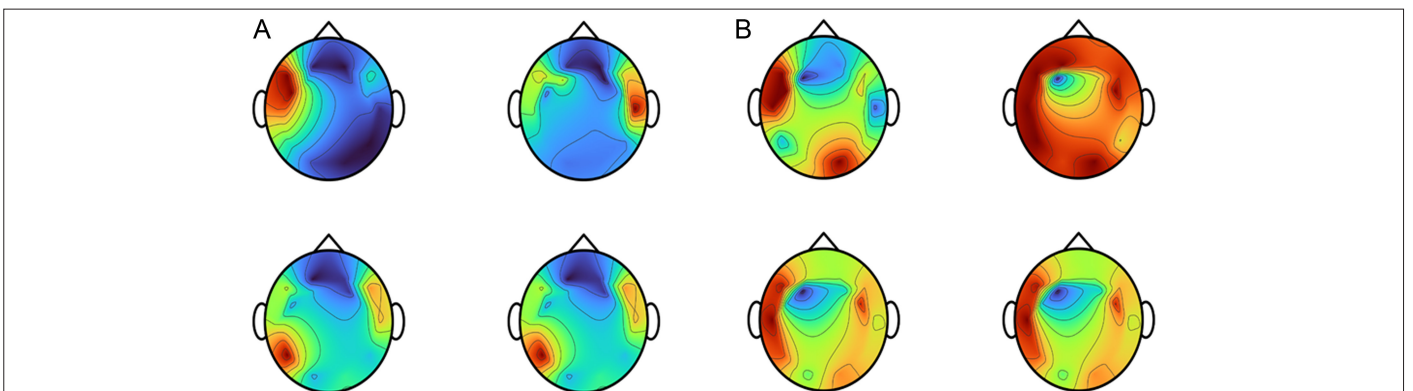

Fig. 3. (a) Concatenated sub-band heat map for a scented case. (b) Concatenated sub-band heat map for an unscented case.

TABLE I. ARCHITECTURE OF THE CONVOLUTIONAL NEURAL NETWORKS MODEL

Layer Type	Output Shape	Number of Parameters
Conv2D	(None, 682, 539, 32)	896
MaxPooling2D	(None, 341, 269, 32)	0
Conv2D	(None, 339, 267, 64)	18496
MaxPooling2D	(None, 169, 133, 64)	0
Flatten	(None, 1438528)	0
Dense	(None, 128)	184131712
Dropout	(None, 128)	0
Dense	(None, 1)	129

III. RESULTS

A. Machine Learning Classification Results
Both total and sub-band power features for all the channels were classified via SVM, k-NN, RF, and NB ML algorithms.

1) Classification With Nonlinear Features
Table II presents the best-performing ML classifiers for nonlinear features used. For each classifier, the average accuracy of all attributes was obtained and is displayed in Table III. Results indicate that the T8 channel has the greatest average accuracy, 73.33%, with the SVM. The average accuracy for the F7 and F4 channels was 72%; meanwhile, the O2 channel reached 69%. O2 has the highest average accuracy with 77.3% with the k-NN classifier, followed by FC6 with 75.33%. Moreover, the AF3, F7, and T8 channels attained an average accuracy of 67%. For NB, F4 has the highest average accuracy of 76.3%, followed by AF4, T8, and FC5 with 72.3%, 70%, and 69% accuracies, respectively.

The average accuracy of the RF classifier for F7 and T8 channels was 68.3% and 70%, respectively. The GB had a 77% accuracy for O2 and T8 channels and a 69.3% accuracy for O1 and F7 channels as the final classifier. Table III also indicates HPs offered the highest accuracy for T8 at 80%, while, the LZC outperformed the others at 93% for the F4 channel using SVM. Using the k-NN classifier, the HPs obtained up to 92% accuracy for the O2 channel and 92% accuracy for the FC6 channel when using the LZC feature.

2) Classification With Relative Sub-band Powers
Considering the previous work of the authors [20], the RF algorithm was shown to be the most accurate and precise of all the classifiers tested, scoring 92% and 93% accuracy and precision, respectively. The accuracy and precision of SVM with a radial basis function kernel, in comparison, have achieved up to 83% and 88%, respectively, while k-NN, where $k = 5$, has reached up to 85%. The best classification performance was shown by the FC6 channel's γ sub-band power, which has an accuracy of 92%.

B. Deep Learning Classification Results
The augmented data was trained for 5 epochs, and Table IV shows the results of the proposed CNN architecture. The accuracy started at 50% and climbed up to 91.6%, while the loss decreased from 22.21 to 0.22. The precision was 49.29% in the beginning and finalized at 89.53%. Finally, the recall value increased to 93.94%.

IV. DISCUSSION

In the authors' previous study, classification with sub-band powers indicated that RF was the most accurate classifier and that the β and γ sub-bands of the F3, F4, and FC6 channels produced the best results [20]. The maximum accuracy for the F4 channel was 86% using all bands, whereas γ and β accuracies were 57% and 50%, respectively. FC6 had 92% accuracy in the γ band, which was followed by 75% accuracy in the β band [20]. Previously, classification with nonlinear features [21] revealed that the best result was 93% accuracy for the F4 channel with the NB classifier. The average accuracy for the F4, F7, O2, and T8 channels was 84.7%, 69.3%, 74.3%, and 76.7%, respectively.

The CNN results given in Table IV show that the network was trained appropriately, as the decrease in loss values was consistent over five epochs. Furthermore, the accuracy reached over 5 epochs outperforms most of the ML classifiers. This indicates that heat maps are an effective way to train CNNs to detect the presence olfactory stimuli in the EEG recordings.

According to the classification results of the nonlinear features given in Table II, T8, O2, F7, and F4 channels gave the highest accuracy results. Moreover, HPs, HFDs, and LZC features produced consistent results across different classifiers, as can be seen in Table III. On the other hand, the LZC feature provided better results consistently across all EEG channels. Since LZC can calculate the temporal complexity of a signal, it emerged as a prominent feature in this study. The CNN accuracy was 91.6%, while the best result of the sub-band

TABLE II. BEST-PERFORMING CLASSIFIERS FOR ALL NONLINEAR FEATURES

Classifier	NB				RF				GB			
EEG Channel/ Performance Metric	Accuracy	Precision	Recall	F-1 Score	Accuracy	Precision	Recall	F-1 Score	Accuracy	Precision	Recall	F-1 Score
F4	**0.93**	**0.92**	**0.94**	**0.93**	0.79	0.78	0.74	0.75	0.79	0.78	0.74	0.75
F7	0.58	0.61	0.58	0.56	0.75	0.76	0.75	0.75	0.75	0.76	0.75	0.75
O2	0.69	0.75	0.78	0.69	**0.85**	**0.83**	**0.89**	**0.84**	0.69	0.75	0.78	0.69
T8	0.8	0.83	0.83	0.8	0.7	0.7	0.71	0.7	0.8	0.83	0.83	0.8

NB, naïve Bayes; RF, random forest; DT, decision tree; GB, gradient boost.

TABLE III. BEST CLASSIFIER PERFORMANCES FOR ALL NONLINEAR FEATURES

Feature	Channel/Classifier	SVM	k-NN	NB	RF	DT	GB
HPs	F4	0.79	0.79	0.79	**0.86**	0.71	0.79
	F7	0.75	0.75	0.75	0.75	0.58	0.75
	O2	0.69	0.92	0.62	0.77	0.69	**0.92**
	P8	0.64	0.64	0.57	0.71	**0.79**	**0.79**
	T8	0.8	0.7	**0.8**	0.7	0.6	**0.8**
HFD	AF3	0.66	**0.83**	0.5	**0.83**	0.83	**0.83**
	AF4	0.66	0.67	0.75	**0.83**	0.83	0.75
	F7	**0.75**	0.75	**0.75**	0.67	0.67	**0.75**
	T8	0.7	0.7	0.7	**0.8**	**0.8**	**0.8**
LZC	AF4	**0.75**	0.66	**0.75**	**0.75**	0.58	0.67
	F4	**0.93**	0.86	0.86	**0.93**	0.64	0.71
	FC6	0.58	**0.92**	0.67	0.58	0.67	0.67
	O2	**0.77**	**0.77**	**0.77**	**0.77**	0.69	**0.77**
	T8	**0.7**	0.6	**0.7**	**0.7**	0.5	0.5

SVM, support vector machine; k-NN, k-nearest neighbors; NB, naïve Bayes; RF, random forest; DT, decision tree; GB, gradient boost.

TABLE IV. CONVOLUTIONAL NEURAL NETWORK CLASSIFIER RESULTS

Epoch	Accuracy	Precision	Recall	Loss
1	0.5	0.4929	0.5227	221.461
2	0.5746	0.5643	0.5985	0.6872
3	0.7929	0.8097	0.7576	0.5253
4	0.8377	0.8365	0.8333	0.3614
5	**0.9160**	**0.8953**	**0.9394**	**0.2213**

power classification was 92% accuracy for the RF classifier. Although the results of the CNN seemed superior to those of the ML classifier, it should be noted that the number of samples was limited in the case of the DL classification. Thus, different sub-bands such as α, β, and γ

were fused to augment the data so that the CNN could be trained better.

Considering the results provided in Table II, the best discriminating channel for olfactory stimulus is F4. This supports previous studies such as, [29] as the orbitofrontal cortex is a tertiary olfactory structure. Thus, it is demonstrated that it is more effective to focus on EEG channels related to the orbitofrontal cortex, such as F4, to detect olfactory stimuli when training artificial intelligence classifiers.

Table V provides a comparison with the previous notable studies, such as [4], [9], and [10] the proposed methods in this study, which produced on-par and better results depending on the compared aspect, such as the significance of the channel or features. Since in this study the data is collected from far more people than in the previous studies, it can be argued that the results of this study generalize better than the previously published ones.

TABLE V. COMPARISON OF RESULTS WITH PREVIOUS WORKS

Study	Dataset Size	Features Used	Classification Type	Classifier	Accuracy Results
[2]	14 Subjects	PSD, ApEn	Odor Identification	k-NN, SVM, XGBoost	77.6%
[4]	5 Subjects	HFD, LLE, ApEn, LZC	Subject-specific Cross-subject	LDA	92.75% 86.9%
[9]	5 Subjects	EEG Sub-band Powers	Subject-specific Cross-subject	SVM	≈50.0%–100.0% ≈50.0%–100.0%
[10]	5 Subjects	EEG Sub-band Powers, Statistical data, HP, Autoregressive Model	Odor Identification Subject Identification	k-NN, NB	52.95%–99.34% 47.68%–97.48%
Proposed Method	33 Subjects	EEG Sub-band Power Heatmaps	Odor Identification	CNN	91.60%

V. CONCLUSION

This research examined how EEG signals can be used to identify olfactory stimuli in the brain. First, the nonlinear features HA, HM, HC, HFD, and LZC were classified using conventional ML classifiers. Then, sub-band powers were categorized using a CNN architecture in comparison to the authors' previous work, in which sub-band powers were classified directly as a 1D series. It should be noted that the nonlinear features and sub-band powers were also compared to assess the effectiveness of nonlinear features. Moreover, to evaluate the efficacy of nonlinear features, the nonlinear features and sub-band powers were compared.

Overall, LZC complexity was found to be the most prominent feature in classifying the presence of olfactory stimuli, highlighting its ability to calculate the temporal complexity of a signal. Another finding is that EEG channels related to the orbitofrontal cortex are more discriminative than others, such as the F4 channel. Moreover, to the best of the authors' knowledge, CNN classification of the heat maps to detect olfactory stimulus was not done by any other researchers previously. This study demonstrates that topographic heat maps can represent the response of the brain to olfactory stimuli accurately.

In future studies, further parameter optimization of the ML classifiers and the CNN will be done utilizing different searching algorithms. The layer structure of the CNN used will also be further exploited to better suit the data and improve the classification performance. Additionally, several other DL methods, such as transfer learning, will be used to classify the heat maps to investigate their effectiveness in terms of olfactory stimulus detection.

Peer-review: Externally peer-reviewed.

Author Contributions: Concept – B.A., S.P.A., R.S, A.A.; Design – S.P.A., R.S.; Supervision – A.A., S.U.; Funding – R.S., A.A.; Materials – R.S., A.A.; Data Collection and/or Processing – B.A., S.P.A., R.S.; Analysis and/or Interpretation – B.A., S.P.A.; Literature Review – B.A., S.P.A.; Writing – B.A., S.P.A, A.A.; Critical Review – A.A., S.U.

Declaration of Interests: The authors have no conflict of interest to declare.

REFERENCES

1. M. Cabanac, "What is emotion?," *Behav. Processes*, vol. 60, no. 2, pp. 69–83, 2002. **[CrossRef]**
2. M. S. Seet *et al.*, "Wearable EEG entropy and spectral measures for classification of consumer reward-based evaluation of odor stimuli," 2021 43rd Annual International Conference of the IEEE Engineering in Medicine & Biology Society (EMBC), 2021. **[CrossRef]**
3. A. Bazzani, S. Ravaioli, L. Trieste, U. Faraguna, and G. Turchetti, "Is EEG suitable for marketing research? A systematic review," *Front. Neurosci.*, vol. 14, 594566, 2020. **[CrossRef]**
4. K. Ezzatdoost, H. Hojjati, and H. Aghajan, "Decoding olfactory stimuli in EEG data using nonlinear features: A pilot study," *J. Neurosci. Methods*, vol. 341, p. 108780, 2020. **[CrossRef]**
5. H. R. Hou, X. N. Zhang, and Q. H. Meng, "Odor-induced emotion recognition based on average frequency band division of EEG signals," *J. Neurosci. Methods*, vol. 334, p. 108599, 2020. **[CrossRef]**
6. H.-R. Hou, Q.-H. Meng, and B. Sun, "A triangular hashing learning approach for olfactory EEG signal recognition," *Applied Soft Computing*, vol. 118, pp. 108471–108471, 2022. **[CrossRef]**
7. X. N. Zhang, Q. H. Meng, M. Zeng, and H. R. Hou, "Decoding olfactory EEG signals for different odor stimuli identification using wavelet-spatial domain feature," *J. Neurosci. Methods*, vol. 363, p. 109355, 2021. **[CrossRef]**
8. N. I. Abbasi, R. Bose, A. Bezerianos, N. V. Thakor, and A. Dragomir, "EEG-based classification of olfactory response to pleasant stimuli," 2019 41st Annual International Conference of the IEEE Engineering in Medicine and Biology Society (EMBC), 2019. **[CrossRef]**
9. E. Kroupi, A. Yazdani, J.-M. Vesin, and T. Ebrahimi, "EEG correlates of pleasant and unpleasant odor perception," *ACM Trans. Multimedia Comput. Commun. Appl.*, vol. 11, no. 1s, pp. 1–17, 2014. **[CrossRef]**
10. O. Aydemir, "Odor and subject identification using electroencephalography reaction to olfactory," *Traitement Signal*, vol. 37, no. 5, pp. 799–805, 2020. **[CrossRef]**
11. Z. Gao, X. Wang, Y. Yang, Y. Li, K. Ma, and G. Chen, "A channel-fused dense convolutional network for EEG-based emotion recognition," *IEEE Trans. Cogn. Dev. Syst.*, vol. 13, no. 4, pp. 945–954, 2021. **[CrossRef]**
12. A. Craik, Y. He, and J. L. Contreras-Vidal, "Deep learning for electroencephalogram (EEG) classification tasks: A review," *J. Neural Eng.*, vol. 16, no. 3, p. 031001, 2019. **[CrossRef]**
13. Md. A. Rahman, M. S. Uddin, and M. Ahmad, "Modeling and classification of voluntary and imagery movements for brain–computer interface from fNIR and EEG signals through convolutional neural network," *Health Inf. Sci. Syst.*, vol. 7, no. 1, 2019. **[CrossRef]**
14. M. Mahmud, M. S. Kaiser, A. Hussain, and S. Vassanelli, "Applications of deep learning and reinforcement learning to Biological Data," *IEEE Trans. Neural Netw. Learn. Syst.*, vol. 29, no. 6, pp. 2063–2079, 2018. **[CrossRef]**
15. Md. A. Rahman, A. Anjum, Md. M. H. Milu, F. Khanam, M. S. Uddin, and Md. N. Mollah, "Emotion recognition from EEG-based relative power spectral topography using convolutional neural network," *Array*, vol. 11, p. 100072, 2021. **[CrossRef]**
16. G. Xiao, M. Shi, M. Ye, B. Xu, Z. Chen, and Q. Ren, "4D attention-based neural network for EEG emotion recognition," *Cogn. Neurodyn.*, vol. 16, no. 4, 805–818, 2022. **[CrossRef]**
17. T. Higuchi, "Approach to an irregular time series on the basis of the fractal theory," *Phys. D Nonlinear Phenom.*, vol. 31, no. 2, pp. 277–283, 1988. **[CrossRef]**
18. B. Hjorth, "EEG analysis based on time domain properties," *Electroencephalogr. Clin. Neurophysiol.*, vol. 29, no. 3, pp. 306–310, 1970. **[CrossRef]**
19. A. Lempel, and J. Ziv, "On the complexity of finite sequences," *IEEE Trans. Inf. Theor.*, vol. 22, no. 1, pp. 75–81, 1976. **[CrossRef]**
20. S. Pehlivan, B. Akbugday, A. Akan, and R. Sadighzadeh, "Detection of olfactory stimulus from EEG signals for neuromarketing applications," 2022 30th Signal Processing and Communications Applications Conference (SIU), Safranbolu, Turkey, pp. 1–4, 2022. **[CrossRef]**
21. B. Akbugday, A. Akan, S. Pehlivan, and R. Sadighzadeh, "An assessment of linear and nonlinear features for detecting olfactory stimulus in EEG," 2022 Medical Technologies Congress (TIPTEKNO), Antalya, Turkey, pp. 1–4, 2022. **[CrossRef]**
22. C.-T. Shi, "Signal pattern recognition based on fractal features and machine learning," *Appl. Sci.*, vol. 8, no. 8, p. 1327, 2018. **[CrossRef]**
23. C. F. Vega, and J. Noel, "Parameters analyzed of Higuchi's fractal dimension for EEG brain signals," 2015 Signal Processing Symposium (SPSympo), Debe, Poland, 2015, 2015, pp. 1–5. **[CrossRef]**
24. W. Klonowski, E. Olejarczyk, and R. Stepien, "'Epileptic seizures' in economic organism," *Physica A: Statistical Mechanics and its Applications*, vol. 342, no. 3–4, pp. 701–707, 2004. **[CrossRef]**
25. C. M. Gómez, A. Mediavilla, R. Hornero, D. Abásolo, and A. Fernández, "Use of the Higuchi's fractal dimension for the analysis of MEG recordings from Alzheimer's disease patients,", *Med. Eng. Phys.*, vol. 31, no. 3, pp. 306–313, Apr. 2009. **[CrossRef]**
26. M. S. Safi, and S. M. M. Safi, "Early detection of Alzheimer's disease from EEG signals using Hjorth parameters," *Biomed. Signal Process. Control*, vol. 65, p. 102338, 2021. **[CrossRef]**
27. A. Alkan, and M. K. Kiymik, "Comparison of AR and Welch methods in epileptic seizure detection," *J. Med. Syst.*, vol. 30, no. 6, pp. 413–419, 2006. **[CrossRef]**
28. "*Topographic EEG/MEG plot*," Available: www.mathworks.com. https://www.mathworks.com/matlabcentral/fileexchange/72729-topographic-eeg-meg-plot. [accessed: May 17, 2023].
29. Y. Soudry, C. Lemogne, D. Malinvaud, S. M. Consoli, and P. Bonfils, "Olfactory system and emotion: Common substrates," *Eur. Ann. Orl. Head Neck Dis.*, vol. 128, no. 1, pp. 18–23, 2011. **[CrossRef]**

Burak Akbugday received the B.Sc. degree from Zonguldak Bulent Ecevit University, Zonguldak, in 2017 in biomedical engineering. Having worked on the development of hardware and software of embedded systems, mobile and desktop applications as well as signal processing throughout his academic career, he published several related papers. Currently, he works as a research assistant in the Department of Electrical and Electronics Engineering and continues to work on biomedical signal analysis using machine and deep learning methods as a Ph.D. student in Izmir University of Economics.

Sude Pehlivan received the B.Sc. degree from İzmir Katip Celebi University, İzmir, in 2019 in Biomedical Engineering. She completed her undergraduate thesis on defining obstacles on the pedestrian path for visually impaired individuals. She continues to work on biological signal and image processing, and deep learning. Currently, she is a Ph.D. candidate in the İzmir University of Economics' Electrical and Electronics program and works as a research assistant at the İzmir University of Economics' Department of Biomedical Engineering.

Reza Sadighzadeh received the B.Sc. degree from the University of Tabriz, Tabriz in 2000 in Electronics Engineering. He received the M.Sc. degree from the University of Tehran, Tehran in 2008 in Strategic Management. He received an MBA degree from Istanbul University School of Business in 2019. Currently, he is a Ph.D. candidate in Izmir Katip Celebi University, Department of Business Administration. His current research interests include Sensory Marketing, Scent Marketing, and Neuromarketing.

Aydin Akan received the B.Sc. degree from the University of Uludag, Bursa, in 1988, the M.Sc. degree from the Technical University of Istanbul, Turkey in 1991, and the Ph.D. degree from the University of Pittsburgh, Pittsburgh, PA, USA, in 1996, all in Electronics Engineering. He has been with the Department of Electrical and Electronics Engineering, Istanbul University between 1996 and 2017, where he was granted the Associate Professor position in 2001, and the full Professor position in 2006. He was appointed as Professor and Chair of the Department of Biomedical Engineering, Izmir Katip Celebi University between March 2017 and January 2020 where he served as the Dean of the School of Engineering and Architecture. Currently, he is a Professor and Chair of the Department of Electrical and Electronics Engineering, Izmir University of Economics. His current research interests include non-stationary signal processing, time-frequency signal analysis, and machine learning methods applied to wireless communications and biomedical engineering. He is a senior member of the IEEE Signal Processing (SP) and Engineering in Medicine and Biology (EMB) Societies, Chair of IEEE-EMB Turkey Section, and Chair of the European Signal Processing Association (EURASIP) Biomedical Image and Signal Analytics (BISA) Technical Area Committee. He is an Associate Editor of the Elsevier Digital Signal Processing Journal.

Sevtap Unal is a Professor of Marketing in the Economics and Business Administration Faculty at Izmir Katip Celebi University in Turkey. During 2015-2016, she was a visiting Professor at the University of Texas at Dallas. Her research interests lie in the areas of consumer behavior, consumer psychology, and marketing research. She has published numerous books, articles, and conference papers in national and international journals and conferences. She serves as editor and reviewer for national and international journals. In addition to her 17 years of teaching experience, she has also participated in consulting and training projects.